Piotr Paplicki
West Pomeranian University of Technology, Szczecin

FIELD CONTROLED AXIAL-FLUX PERMANENT-MAGNET MACHINE

MASZYNA TARCZOWA Z MAGNESAMI TRWAŁYMI I REGULOWANYM WZBUDZENIEM

Abstract: This paper presents the concept of an innovative field-controlled axial-flux surface-mounted permanent-magnet machine. To show the work principle and applicability of a idea of air-gap flux control the dual-rotor with inner slotted stator machine is investigated and analyzed in detail using tree-dimensional finite-element analysis (3D-FEA). The control range, back EMF, torque output and cogging torque component have been evaluated.

Streszczenie: Artykuł przedstawia koncepcję maszyny tarczowej z magnesami trwałymi mocowanymi powierzchniowo i regulacją wzbudzenia. W celu przedstawienia zasady działania i możliwości zastosowania idea regulacji strumienia wzbudzenia opracowano i poddano analizie polowej trójwymiarowy model maszyny z wirnikiem dwutarczowym i wewnętrznym żłobkowym stojanem. Wyznaczono zakres regulacji wzbudzenia, napięcia indukowanego w uzwojeniach stojana i momentu obrotowego oraz moment zaczepowy.

Keywords: *axial-flux electrical machine, permanent magnet, magnetic field control, finite-element analysis*
Słowa kluczowe*: maszyna elektryczna o strumieniu osiowym , magnes trwały, sterowanie polem magnetycznym , analiza metodą FE*

1. Introduction

Nowadays permanent magnet (PM) machines have been used in a wide range of applications. Motor efficiency is improved, and higher power density is achieved. Although conventional radial-flux PM machines (RFPM) are the most widely used type of PM machines, axial-flux (AFPM) machines have been gaining popularity in applications where the used conventional machines are not appropriate, such as hybrid traction motors and generators. They can be designed for higher torque-to-weight ratio, better efficiency and lower noise and vibration levels. However, the main drawback of AFPM machines arises from the area of field weakening. Advances in material technology have allowed to arrive at new machine configurations in order to achieve flux weakening in a simple manner.

There presently exist a number of alternative solutions to eliminate this problem in radial and axial-flux machines.

This paper aims to address the field-weakening constructions in AFPM machines by suggesting an idea of air-gap flux control. The idea can be easily applied to any axial-flux machine, including multiple structures.

To show the application of the idea, the machine with flux control dual-rotor and single-stator (FCAFPM) is chosen and analyzed using the finite element analysis (FEA).

2. Structure and principles of FCAFPM machine

Airgap flux control technique for one pole pair section in a simple PM rotor with the *dc* control coil on the stator of is presented in Fig. 1.

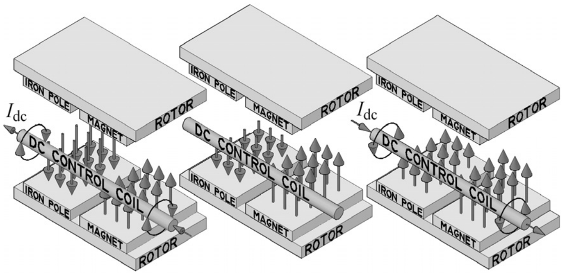

$I_{dc} < 0$ $I_{dc} = 0$ $I_{dc} > 0$

Fig. 1. Method of field-weakening and strengthening in PM machines with positive (right) and negative (left) dc fields

Unlike the conventional *d*-axis current injection field-weakening technique, *dc* field winding control is used to slight polarization of the rotor iron poles . In accordance with the magnitude and direction of the excitation current, the air-gap flux across the pole section can be increased or reduced. The air-gap flux densities resulting from different *dc* excitation acting on the double sided machine stator winding, according to Fig. 2c, become different and the induced EMF is reduced or increased.

The stator and rotor structures of the FCAFPM machine are shown in Fig. 2. The stator is formed by sheet steel toroidal core, circumferentially wound *dc* field winding and two sets of three-phase windings. The *dc* field winding is placed inside the hole of the slotted stator core between the inner stator end-winding.

The machine rotor is formed by two magnetic rotor disks, arc-shaped iron pieces, arc-shaped axially magnetized NdFeB magnets mounted on the surfaces of the two rotor disks, magnetic tube made from SMC material and a shaft. It should be pointed out that a rotor pole is formed by PM and iron pole piece and there exists some space between them in order to lessen the leakage.

The main motor dimensions and parameters are presented in Table 1.

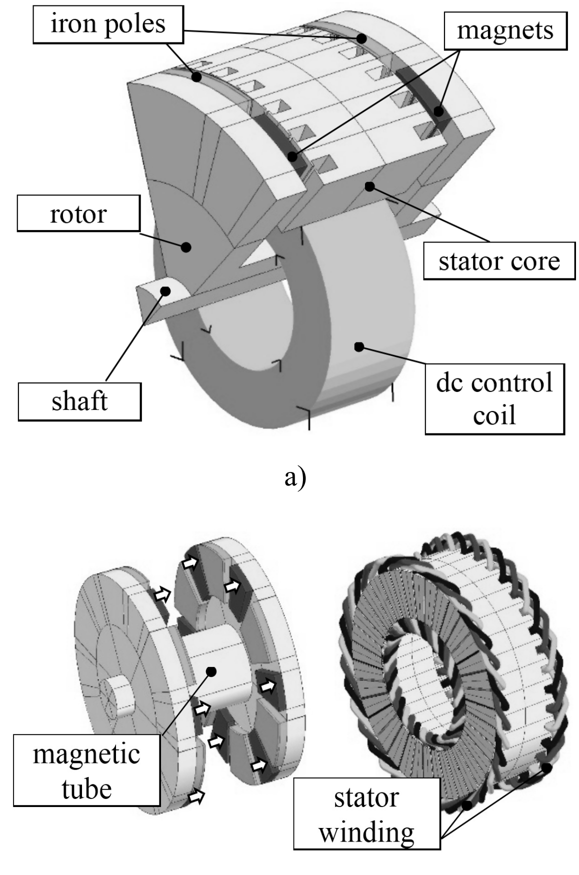

a)

b) c)

Fig. 2. 3D FEM model structure of FCAFPM *machine –a); rotor parts –b); stator parts –c)*

Table 1. The main date of the analyzed FCAFPM machine

Number of poles	12
Magnet type	NdFeB
Magnet B_r	1.2 T
Magnet permeability	1.05
Stator outer diameter	240.0 mm
Stator inner diameter	140.0 mm
Airgap iron pole/PM	0.5/2.5mm
PM length	8.0 mm
Iron pole length	10.0 mm
Stator axial length	80.0 mm
Rotor disc axial length	20.0 mm
Number of slots	36
Width of the slot opening	2.0 mm

The *dc* field winding can weaken or strengthen the air-gap flux, depending on the direction of the field current (I_{dc}). Figures 3 and 4 show the air-gap flux density for zero (I_{dc}=0), positive (I_{dc}>0) and negative (I_{dc}<0) *dc* field current cases. As can be seen from the plots, the air-gap flux in front of the iron pole changes its direction and magnitude, depending on the direction of the *dc* field current. Since the PM flux change slightly with the field current, the total flux in the air-gap alters with the direction of the *dc* field current and the magnitude.

Figure 3 shows the 2-D flux density distribution over one magnet and iron pole section of the rotor for three different cases of the *dc* field current and proves the principles of the air-gap flux control. It should be pointed out that field current I_{dc}≠0 corresponds to *dc* control coil current density equal j_{dc} =5A/mm^2. The slotting effects of the machine stator are monitored from the three parts of the figure 4.

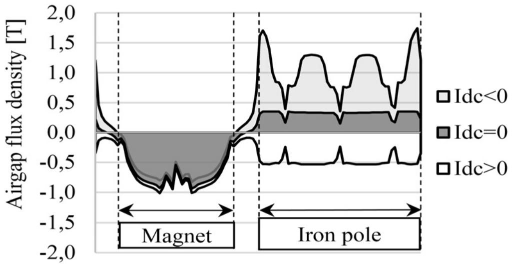

Fig. 3. Two-dimensional air gap flux density distribution for different values of the dc field current over magnet and iron pole

Moreover it should be noted that the flux boosting is limited both by the current density of the *dc* field and the iron saturation mainly. Figure 5 shows the magnetic flux distribution within

3D-FEM model of FCAFPM machine for different polarities and values of *dc* field current.

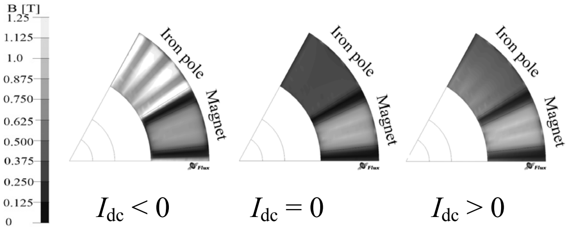

$I_{dc} < 0$ $I_{dc} = 0$ $I_{dc} > 0$

Fig. 4. Air-gap flux density distribution for different values of the dc field current over magnet and iron pole

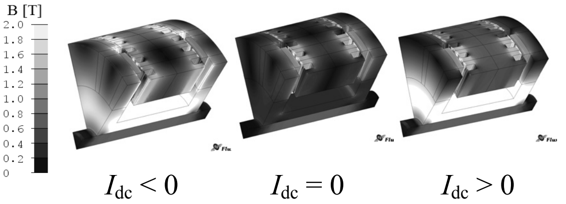

$I_{dc} < 0$ $I_{dc} = 0$ $I_{dc} > 0$

Fig. 5. Rotor and stator magnetic flux distribution for different dc field current

3. No-load characteristics

The air-gap flux can be thought of as the combination of magnet flux and iron flux due to *dc* field winding. Figure 6 shows the air-gap flux components: magnet flux, iron pole flux and total flux values over one pair of poles at no load as the *dc* field current varies.

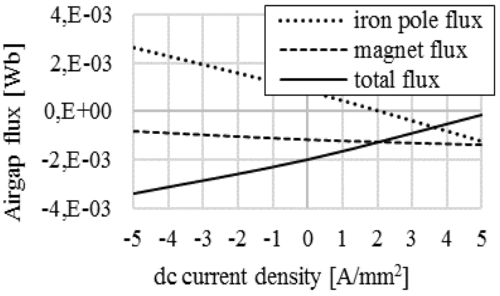

Fig. 6. Air-gap PM, iron and total flux of the machine over one pair pole of machine

Each component of the airgap flux is obtained using 3D-FEA. As can be seen from the Fig. 6, the total air-gap flux can be weakened or strengthened with respect to the zero *dc* current case. With the variation of ±6500 Ampere-turns, the air-gap flux control range at no load becomes roughly 71% with field-strengthening and 93% with field-weakening. This way a reasonable range of field weakening can be obtained with reasonable *dc* field current.

Figure 7 shows the back EMF of the model machine under various field strengths.

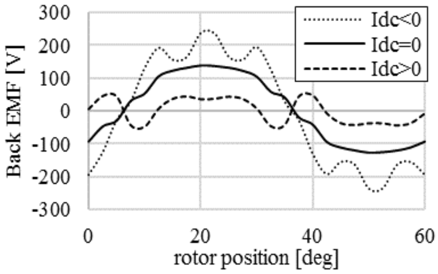

Fig. 7. Back EMF waveform for different values of the dc field current at 1000 rpm

A significant field control capability is clearly observed. Attention should be drawn to the ratio of the EMF values that are changed from the maximum value to the minimum value. According to simulation FEA results contained in table 2 it can be concluded that the field-weakening ratio of 4:1 and higher can be obtained.

Table 2. Back EMF values in Volts at different dc field current

	$I_{dc} < 0$	$I_{dc} = 0$	$I_{dc} > 0$
EMF(rms)	163.8	99.5	34.7
EMF(av)	150.6	91.6	37.1

Electromagnetic torque characteristics of the machine as a function of *dc* field current and armature currents are shown in Fig. 8.

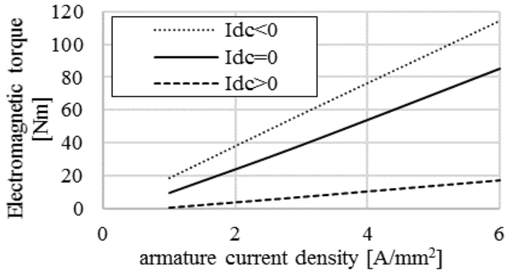

Fig. 8. Electromagnetic torque for different values of the dc field current

As can be seen from these static torque characteristics, machine torque increases as the armature current increases. Peak torque variation against armature current for a given *dc* field current is close to linear.

With the variation of armature current density j_a=1÷6 A/mm^2, the electromagnetic torque control range at load becomes roughly 35% with strengthening field and 80% with weakening field.

Figure 9 shows the cogging torque which is one of the most important sources of torque pulsations in PM machines. It can be minimized using various techniques.

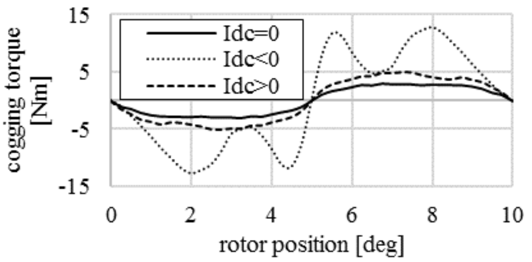

Fig. 9. Cogging torque for different values of the dc field current

The cogging torque has a peak value of 3.0 Nm for $I_{dc}=0$ which is roughly 4 % of the predicted machine rated torque 70 Nm. In other cases cogging torque has a peak value of 12.7 Nm for $I_{dc}<0$ and 5.0 Nm for $I_{dc}>0$.

4. Conclusion

The novel concept of air-gap flux control in both weakening and strengthening regions has been introduced for axial-flux surface mounted PM machines.

The 3D FEA of the topology has been illustrated for different field currents to prove the flux weakening and strengthening concept. It was found out that a reasonable range of field weakening can be obtained with practical *dc* field currents. The control range, back EMF, torque output and cogging torque component have also been analyzed. It has been demonstrated that the idea allows an easy control of the axial-gap machine without any negative effects of current injection. This concept of machine is one of the PM-machine which is capable of true field weakening.

6. Bibliography

[1] Ki-Chan K.; A.: *Novel Magnetic Flux Weakening Method of Permanent Magnet Synchronous Motor for Electric Vehicles*. IEEE Transactions on Magn., vol.48, no.11, 2012, pp.4042-4045

[2] May H., Palka R., Paplicki P., Szkolny S., Canders W.-R.: *Modified concept of permanent magnet excited synchronous machines with improved high-speed features*. Archives of Electrical Engineering, 4 (2011), pp. 531-540

[3] Zhu X., Quan L., Chen D.: *Design and Analysis of a New Flux Memory Doubly Salient Motor Capable of Online Flux Control*. IEEE Trans. Magn., vol. 47, no. 10, Oct. 2011, pp. 3220-3223

[4] Kosaka T., Sridharbabu M., Yamamoto M., Matsui N.: *Design studies on hybrid excitation motor for main spindle drive in machine tools*. IEEE Trans. Ind. Electron., no. 11/2010, pp. 3807–3813

[5] Chaithongsuk S., Nahid-Mobarakeh B., Caron J., Takorabet N., Meibody-Tabar F.: *Optimal Design of Permanent Magnet Motors to Improve Field-Weakening Performances in Variable Speed Drives*. IEEE Transactions on Industrial Electronics, vol.59, no.6, June 2012, pp.2484-2494

[6] Laskaris K.I., Kladas A.G.: *Optimal Power Utilization by AdjustingTorque Boost and Field Weakening Operation in Permanent Magnet Traction Motors*. IEEE Transactions on Energy Conversion, vol.27, no.3, Sept. 2012, pp.615-623

[7] May H., Palka R., Paplicki P., Szkolny S., Wardach M.: *Comparative research of different structures of a permanent-magnet excited synchronous machine for electric vehicles*. Electrical Review, R. 88 NR 12a/2012, pp.53-55

[8] Di Barba P., Mognaschi M. E., Palka R., Paplicki P., Szkolny S.: *Design optimization of a permanent-magnet excited synchronous machine for electrical automobiles*. International Journal of Applied Electromagnetics and Mechanics, IOS Press, vol.39, Number 1-4/2012, pp.889-895

[9] Aydin M.; Surong H., Lipo, T.A.,: *Design, Analysis, and Control of a Hybrid Field-Controlled Axial-Flux Permanent-Magnet Motor*. Industrial Electronics, IEEE Transactions on Magn., vol.57, no.1, Jan. 2010, pp.78-87

[10] Paplicki P.: *Bezrdzeniowa maszyna tarczowa z magnesami trwałymi-modelowanie 3D*. Przegląd Elektrotechniczny, R. 87, nr 11, 2011, s. 106–110

[11] Paplicki P.: *Maszyna tarczowa z magnesami trwałymi – wybrane aspekty budowy parametrycznych modeli geometrycznych 3D*. Zeszyty Problemowe – Maszyny Elektryczne, 93/2011 s.167-171

[12] Putek P., Slodička M., Paplicki P., Pałka R.: *Minimization of cogging torque in permanent magnet machines using the topological gradient and adjoint sensitivity in multi-objective design*. International Journal of Applied Electromagnetics and Mechanics Vol. 39, nr 1-4 (2012), s. 933-940

[13] Putek P., Paplicki P., Slodička M., Pałka R., Van Keer R.: *Application of topological gradient and continuum sensitivity analysis to the multi-objective design optimization of a permanent-magnet excited synchronous machine*. Przegląd Elektrotechniczny, R. 88, nr 7a (2012), s. 256-260

Author

dr inż. Piotr Paplicki, Department of Power Systems and Electrical Drives, West Pomeranian University of Technology, ul. Sikorskiego 37, 70-313 Szczecin, Poland, e-mail: piotr.paplicki@zut.edu.pl.

Acknowledgement

This work was supported by the Ministry of Education and Science, Poland, under grant N N510 5080406.

Reviewer

prof. dr hab. inż. Bronisław Tomczuk